



Initiation of Motion for Sand-Mud Bed Types

P. S. Miranda^{1,2}(✉), J. J. van der Werf^{1,2}, and S. J. M. H. Hulscher¹

¹ University of Twente, 7522 NB Enschede, The Netherlands
p.s.miranda@utwente.nl

² Deltares, Boussinesqweg 1, 2629 HV Delft, The Netherlands

Abstract. The initiation of motion of sand-mud bed mixtures remains inadequately understood and not accurately predicted. This study sought to compare and analyze the methodology and results of different sand-mud erosion experiments. Data from different erosion experiments were combined to create a dataset of varying sand-mud combinations with an emphasis on varying clay-silt ratios. The framework proposed by Van Ledden [1] was used to separate the data into six different bed types. These bed types are characterized by their cohesive property and network structure. The cohesive property is based on the mass fraction of clay and the network structure is based on the dominant sediment fraction. The different bed types demonstrated different ranges of critical bed shear stress for various ranges of median grain size or mass fraction of mud. This indicates that distinct initiation of motion mechanisms are dominant in different bed types.

Keywords: sand-mud · initiation of motion · sediment transport

1 Introduction

Sand-mud is a ubiquitous type of sediment in estuaries and deltas. Estuaries and deltas function as locations for global ports around the world and as vital habitat for marine ecology. Analyzing the properties of sand-mud mixtures, particularly its erosion potential, facilitates in the planning and management of these systems.

Sand-mud erosion occurs in different modes (e.g. particle, surface, and mass erosion) as discussed by van Rijn [2]. However, identifying the initiation of motion remains without quantifiable standards. As a result, recent sand-mud erosion experiments continue to use different methods.

The proposed mathematical models for sand-mud initiation of motion, denoted by the critical bed shear stress parameter or τ_{crit} , have been developed based on available sand-mud data from researchers developing those models. These equations describe the initiation of motion of sand-mud beds through bulk parameters, such as median grain size diameter, d_{50} , or mass fraction of mud, P_{mud} . However, mud is composed of silt and clay. Clay particles are naturally cohesive while silt particles exhibit apparent cohesion due to their reduced permeability. At present, initiation of motion equations for sand-mud mixtures do not account for different quantities in silt and clay.

To date, an erosion experiment using wide variations in sand-silt-clay combinations has not been undertaken. As a result, the analysis of the initiation of motion of sand-mud beds with different mud fractions using large variations in silt and clay quantities has not been done. However, recent erosion experiments have been performed with limited but different ranges of clay-silt combinations.

This study was conducted to combine the results of sand-mud erosion experiments that used various clay-silt ratios through an analysis of methodologies. This study also examined a framework that highlights the contribution of each sediment fraction in the initiation of motion process. This paper is organized as follows. Section 2 explains the methodology used in the selection of data and framework. Section 3 lists the erosion experiments whose results are included in the combined dataset and the application of the chosen framework to the combined dataset. Section 4 gives conclusions on the created dataset and implications of applying the selected framework.

2 Data and Framework Selection

The methodology for dataset selection needed criteria to assess the discrepancies in methods between different erosion experiments. The methodology for framework selection needed to isolate the different sediment fractions based on physical characteristics.

2.1 Data Selection

The selection process defined criteria to analyze methodologies and results across erosion experiments. Datasets from erosion experiments using sediment less than 2 mm were used. The definition of each sediment fraction was based on their cohesive properties (sand: non-cohesive; silt: apparently cohesive; clay: cohesive) and grain size diameter. Specifically, the grain size diameter definition has the diameter lower limit of sand at 63 μm and the diameter upper limit of clay at 2 μm . Furthermore, datasets must have reported measured bulk geotechnical parameters such as water content, and bulk density. Next, a criterion for experimental setups limited the selection to those that used unidirectional flow since this type of forcing replicates the tidal forcing in estuaries. The method of obtaining derived parameters was also reviewed to ensure that parameters such as bed shear stress were similarly calculated. The derivation of bed shear stress from erosion experiments lacks a standardized methodology, therefore, multiple methods were accepted. Such methods included experiments that derived bed shear stress from law of the wall velocity profiles or experiments that estimated from the measured near-bed turbulence. A more subjective derived parameter is the τ_{crit} or the bed shear stress at initiation of motion. Similar to bed shear stress, there is no standard definition for determining τ_{crit} . Consequently, multiple methods were also deemed accepted. These methods included: visual observation, extrapolation from the relationship between erosion rate and bed shear stress, a threshold erosion rate, and a threshold suspended sediment concentration value. These criteria did not yield an absolute like-for-like comparison across sand-mud erosion experiments. However, the criteria provided a dataset with a large variation in sand-mud composition, bulk geotechnical parameters, and initiation of motion information.

2.2 Framework

The work by Van Ledden [1] proposed a framework delineating the erosion behavior of sand-mud that accounts for each sediment fraction. The framework categorizes according to 2 characteristics: cohesion and network structure. Cohesion is based on the empirically observed threshold for mass fraction of clay or P_{clay} . Sand-mud is considered cohesive with $P_{clay} \geq 5\text{--}10\%$. In subsequent analyses, this threshold is set at 7%. Network structure refers to the sediment fraction that may or may not form a network of particles within the sand-mud bed. From fluidization experiments, sand particles form a network when the volume fraction of sand, ϕ_{sand} , exceeds 40%. Similarly, silt particles form a network when the volume fraction of silt, ϕ_{silt} , exceeds 40% of the pore volume around sand particles. In contrast and due to the cohesive nature, a clay-water matrix is formed instead of a clay network. This matrix is present when sand-mud bed is neither sand- or silt-dominated, and cohesive. Finally, a mixed network is formed when neither sand nor silt form a network and the bed is non-cohesive. A mixed network is characterized as having contributions from all sediment fractions. The proposed framework results in six bed types: (I) sand-dominated non-cohesive, (II) sand-dominated cohesive, (III) mixed network non-cohesive, (IV) clay-water matrix cohesive, (V) silt-dominated non-cohesive, and (VI) silt-dominated cohesive. The framework is adopted to describe the initiation of motion based on cohesion and dominant network structure of a sand-mud bed type.

3 Results

3.1 Selected Datasets

After applying the proposed criteria, the following datasets provided a wide range of sand-mud compositions with sufficient experimental and geotechnical information.

The work by Jacobs [3, 4] investigated sand-mud erosion using artificially created sand-mud based on clay-silt ratios between 0.04–0.44 and sand-silt ratios between 0.31 and 18.6.

The work at the US Army Corp of Engineers [5] investigated the erosion thresholds of sand-mud using both artificial and natural sand-mud. The sediment had mud content from 0 to 100% with different types of clay. Experiments were conducted using purely Kaolinite. Other experiments were conducted using a combination of Kaolinite and Bentonite. While another set of experiments used mud taken from the Mississippi river.

The previous two datasets provided data containing mud with significant clay content. It was necessary to find datasets that conducted erosion experiments for mud with low clay content ($P_{clay} < 7\%$). Part of the PhD work by te Slaa [6] was useful in filling this gap in data since the PhD work focused on the erosion of silt-rich environments. In this dataset, the clay content was 0 while the silt content was between 90–100%.

Another erosion experiment that focused on the behavior of silt-dominated systems is the work by Yao [7]. The recalculated P_{silt} of the sediment samples range from 20–82% while P_{clay} was approximately 0%. This dataset provided additional samples with significant silt content and insignificant amounts of clay content.

Finally, the dataset from the MuSa project in Deltares [8] collected and tested sand-mud samples from within the Netherlands and from sites abroad. The range of sand-silt-clay composition had mud content between 12–95%, and composed of different clay-silt ratios, 0.19–0.76.

The geotechnical information provided in the experiments were not consistently reported. To complete the information, known geotechnical relationships were used to calculate for any gaps. In the end, it was imperative that median grain size diameter, (d_{50} , m), water content ($W\%$), volume fraction of water (ϕ_{water}), dry bulk density (kg/m^3), and bulk density (kg/m^3) were known or calculated for each data point.

In total, the dataset contains 107 data points. This dataset has different combinations of sand and mud as well as sufficient data containing different types of mud.

3.2 Bed Type Classification

The framework proposed by Van Ledden is applied to the collected datasets. The results are shown in Fig. 121.1: 54 datapoints in bed type I, 3 datapoints in bed type II, 13 datapoints in bed type III, 25 datapoints in bed type IV, 12 datapoints in bed type V, and 0 datapoints in bed type VI. Despite the absence of data in bed type VI, the result of applying the framework provides an opportunity to investigate parameters and processes in bed types I to V.

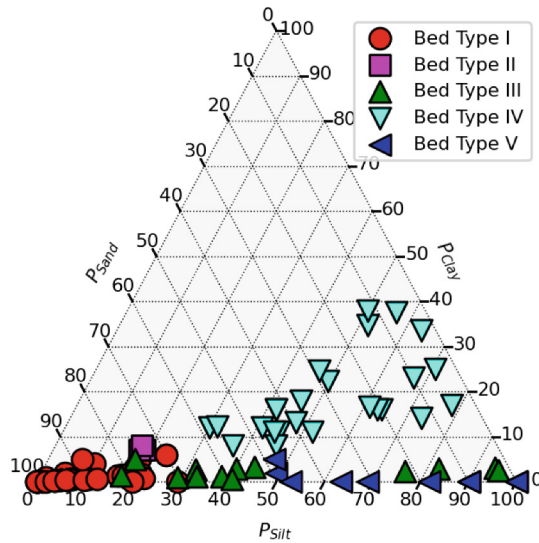


Fig. 121.1. Ternary diagram showing the spread of data from the datasets that fulfilled the selection criteria. Each data point is marked and colored according to its Van Ledden bed type [1].

Classification of sand-mud into different bed types shows its effect on the range of τ_{crit} . Figure 121.2 shows a plot of each bed type in terms of its τ_{crit} against d_{50} and

volume fraction of mud, P_{mud} . Bed type I has the largest d_{50} and lowest P_{mud} with a wide range of τ_{crit} between 0.1–2.4 Pa. Despite limited datapoints, bed type II has smaller d_{50} but larger P_{mud} than bed type I with a narrower range of τ_{crit} between 0.9–1.0 Pa. Bed types III and IV have a large spreads of d_{50} 's and of critical bed shear stresses despite containing the same fraction of mud. Bed type III shows that an increase in P_{mud} may result in an increase in τ_{crit} . Conversely, bed type IV appears to decrease in τ_{crit} with increasing P_{mud} . Finally, bed type V does have a large range of d_{50} but its τ_{crit} values are, on average, comparable to the values of pure sand. The bed types with different cohesive and network structure properties are shown to affect the magnitude and spread of τ_{crit} across d_{50} and P_{mud} .

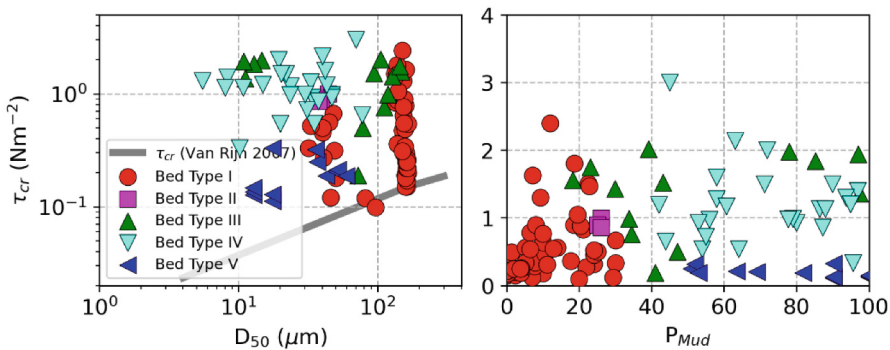


Fig. 121.2. Left plot presents d_{50} and τ_{crit} . Data points are colored according to bed type [1]. The τ_{crit} of pure sand from van Rijn [9] is also plotted for reference. Right plot presents the τ_{crit} as P_{mud} varies. The data points are similarly colored [1].

This classification helps identify which mechanisms may be relevant during the complex initiation of motion process. The complexity is evident in the different forms of proposed critical shear stress equations [9, 10, 11]. Using a framework helps reduce complexity by classifying sand-mud mixtures on a physical basis. In this classification, a better understanding of the controlling factors for different sand-mud combinations can be done. Furthermore, 1st order equations can be estimated based on the subdivision. These can serve as guidelines for future erosion experiments or analyses.

4 Conclusions

The objective of this study was to build a dataset with a large spectrum of sand-silt-clay combinations from various erosion experiments in an attempt to obtain like-for-like comparisons between experimental setups and results. This objective was sought in lieu of performing erosion experiments with different mud content using a large variation in clay-silt ratios. Since there is no standardized methodology for measuring parameters, an absolute fair comparison was not achieved. This is especially true for derived parameters such as bed shear stress and critical bed shear stress. Nevertheless, the selection of

methods and reported sediment information are reasonable criteria to build a coherent dataset of various sand-silt-clay combinations from different erosion experiments.

The framework proposed by Van Ledden classified this dataset into six bed types based on cohesion and network structure characteristics. This approach avoids hidden or compound effects that is possible in mathematical models that describe initiation of motion based on the variations of a single parameter, such as d_{50} or P_{mud} . This framework reduces the complexity in sand-mud bed initiation of motion using physical characteristics by classifying sand-silt-clay combinations into bed types. The framework also allows subsequent research to focus on parameters dominant in describing processes in initiation of motion per bed type.

Acknowledgements. This study is financially support by the European Union's (EU) Horizon Europe Framework Programme (HORIZON) via SEDIMARE (Grant Agreement No. 101072443), an MSCA Doctoral Network (HORIZON-MSCA-2021-DN-01).

The researchers would like to acknowledge dr. Bas van Maren and Roy van Weerdenburg for their input in sand-mud, and specifically, silt erosion research. The researchers would also like to acknowledge David Perkey, PhD for his generosity in sharing the dataset from the US Army Corp of Engineering report [5].

References

1. Van Ledden M et al (2004) A conceptual framework for the erosion behaviour of sand-mud mixtures. *Cont Shelf Res* 24(1):1–11
2. van Rijn LC (2020) Erodibility of mud–sand bed mixtures. *J Hydraul Eng* 146(1)
3. Jacobs W et al (2011) Erosion threshold of sand–mud mixtures. *Cont Shelf Res* 31(10):S14–S25
4. Jacobs W (2011) Sand-Mud Erosion from a Soil Mechanical Perspective. [Doctoral thesis, Delft University of Technology]
5. Perera C et al (2020) Erosion rate of sand and mud mixtures. *Intl J Sediment Res* 35(6):563–575
6. te Slaa S (2020). Deposition and erosion of silt-rich sediment-water mixtures [Doctoral thesis, Delft University of Technology]
7. Yao P et al (2022) Erosion behavior of sand-silt mixtures: revisiting the erosion threshold. *Water Resour Res* 58(9)
8. Albernaz M B et al (2025) Results of laboratory experiments: Results Phase 1A & B. <https://publicwiki.deltares.nl/display/TKIP/DEL112+-+MUSA>. Accessed 15 Jan 2025
9. van Rijn LC (2007) Unified view of sediment transport by currents and waves. i: initiation of motion, bed roughness, and bed-load transport. *J Hydraul Eng* 133(6):649–667
10. Wu W et al (2018) Critical shear stress for erosion of sand and mud mixtures. *J Hydraul Res* 56(1):96–110
11. Chen D et al (2018) Unified formula for critical shear stress for erosion of sand, mud, and sand–mud mixtures. *J Hydraul Eng* 144(8)

Open Access This chapter is licensed under the terms of the Creative Commons Attribution 4.0 International License (<http://creativecommons.org/licenses/by/4.0/>), which permits use, sharing, adaptation, distribution and reproduction in any medium or format, as long as you give appropriate credit to the original author(s) and the source, provide a link to the Creative Commons license and indicate if changes were made.

The images or other third party material in this chapter are included in the chapter's Creative Commons license, unless indicated otherwise in a credit line to the material. If material is not included in the chapter's Creative Commons license and your intended use is not permitted by statutory regulation or exceeds the permitted use, you will need to obtain permission directly from the copyright holder.

